European Polymer Journal 47 (2011) 925–936

Contents lists available at ScienceDirect

European Polymer Journal

journal homepage: www.elsevier.com/locate/europolj

Macromolecular Nanotechnology

Detailed analysis of dynamic mechanical properties of TPU nanocomposite: The role of the interfaces

Marco Aurilia [a,*], Filomena Piscitelli [b,c], Luigi Sorrentino [b], Marino Lavorgna [b], Salvatore Iannace [b]

[a] IMAST – Technological District on Polymeric and Composite Materials Engineering and Structures, Piazzale Enrico Fermi, 1 – 80055 Località Granatello Portici (NA), Italy
[b] IMCB-CNR – Institute of Composite and Biomedical Materials, Piazzale Enrico Fermi, 1 – 80055 Località Granatello Portici (NA), Italy
[c] DIMP- Department of Materials Engineering and Production – University of Naples "Federico II", Piazzale Vincenzo Tecchio, Napoli 80 – 80125, Italy

ARTICLE INFO

Article history:
Received 15 July 2010
Received in revised form 28 December 2010
Accepted 5 January 2011
Available online 19 January 2011

Keywords:
Thermoplastic polyurethane
Nanocomposites
Microdomain morphology
Dynamic mechanical properties
Small angle X-ray diffraction

ABSTRACT

Organo-modified layered silicates (OMLSs) can largely improve mechanical properties of Thermoplastic polyurethanes (TPUs) as well as affect their microdomain morphology. Nanocomposite TPU containing OMLSs were prepared by melt blending at different concentrations. The addition of OMLS has both induced variation in enthalpy of melting of hard and soft phases, and influenced the glass transition temperature of soft domains, as result of the microdomain phase segregation measured by means of fourier transform infrared spectroscopy (FT-IR). Small angle X-ray scattering (SAXS) analysis has shown that the mean distance between hard domains was mostly unaffected by the filler. However, its distribution broadened with the increasing concentration of the OMLSs, resulting in increased extent of the hard domain interface. The storage modulus of TPU nanocomposites incremented with the silicate content, while the dynamic strain scan tests showed pronounced non linear viscoelastic behavior. The analysis of morphological data obtained by SAXS and FT-IR measurements were correlated to thermal and dynamic mechanical properties of TPU samples suggesting a crucial role of the soft domains interface. The storage modulus and loss tangent of TPU nanocomposites were found to increase with the increasing of the interface area of soft domains with both hard domains and OMLS stacks.

1. Introduction

Thermoplastic polyurethane (TPU) is a block copolymer made up by alternating soft and rigid segments. The hard segments are formed by addition of a chain extender, such as butadiene diol, to the isocyanate (methylene-diphenyl diisocyanate). The soft segments consist of flexible polyether or polyester chains (polyols) connecting two hard segments. The soft and hard segments are incompatible at room temperature and aggregate into soft (SDs) and hard domains (HDs), respectively, resulting in a polymeric system characterized schematically by HDs formed amid the rubbery SDs [1]. However in TPU systems a third phase, the interphase between HDs and SDs, has been studies by some authors [2–4]. The driving forces for the microphase segregation are: the development of crystallinity in the hard segments, the difference in melting points, the segmental polarity difference, segmental length, overall composition and molecular weight. The hard segments have a much higher melting point and polarity than the much less polar and low-melting soft segments [1].

Morphology significantly affects final properties of the TPU. In fact, the size, crystallinity and interconnectivity of the HDs, as well as the nature of domain interface and the mixing of hard segments in the soft segment phase, influence most of physical properties such as elasticity and toughness. SDs form an elastomeric matrix responsible for the elastic properties of TPUs, while HDs act as both

* Corresponding author. Tel.: +39 0817769241; fax: +39 0817760741.
E-mail addresses: aurilia@unina.it, marco.aurilia@imast.it (M. Aurilia).

0014-3057/$ - see front matter © 2011 Elsevier Ltd. All rights reserved.
doi:10.1016/j.eurpolymj.2011.01.005

cross-links and reinforcing fillers. Furthermore both the soft and hard phases may be amorphous or partially crystalline [1]. Indeed, a thorough knowledge of the morphology is essential for understanding the structure–property relationships. HDs can form fibrillar, globular or lamellar structures within continuous soft matrix, or interconnected HD network. Many studies have been focussed at analyzing the HDs structure using several methodologies, such as wide-angle X-ray scattering [5], small-angle X-ray scattering (SAXS) [6–15], atomic force microscope (AFM) [16–19] and FT-IR [20,21].

Recently many authors have reported improvement in TPU properties through addition of variable types of nanofiller (carbon nanofibres, carbon nanotubes, organo-modified silicates, nanosilica) using different preparation techniques, such as in situ polymerization [22–26], melt blending [27–33], solution mixing techniques [34,35], and via solvent-exchange processing [36]. TPU based nanocomposites presented increase in mechanical [23–36], barrier properties [37], tear strength, abrasion resistance [25,29], and thermal stability [37].

Layered silicates can significantly change the microphase domain size and shape of block polymers, delineating a potential route to control morphology on the nanoscale and accordingly to alter the block copolymer properties [38]. Song et al. [22] studied the influence of nanoclay on the polyurethane phase separation with SAXS and AFM, and found that silicates induce phase separation and reduction of domains sizes. Finnigan et al. [39] showed that the addition of 3% by weight of OMLSs in TPU did not result in a significant variation of HDs mean distance whereas changes occured at the polymer-filler interface. The effects of nanofiller on dynamic mechanical properties of TPU nanocomposites have also been studied. Storage modulus of TPU filled with carbon nanofibres has shown a non-linear behavior [40] similar to the Payne effect [41]. This behavior has also been detected in nanocomposite TPU filled with OMLS [27].

In all these studies the effect of nanofiller on phase morphology, thermal and dynamic mechanical properties of TPU have been investigated separately and never directly correlated. In the present work the influence of OMLS on the phase morphology of TPU has been analyzed by means of different techniques (differential scanning calorimetry – DSC, SAXS, FT-IR) and the viscoelastic behavior has been determined through dynamic mechanical analysis (DMA). Consequently the phase morphology variations have been correlated to the viscoelastic behavior of TPU. Furthermore, the analyses of crystallization of SDs in nanofilled TPU samples provided a sound tool to asses the influence of the phase morphology on dynamic mechanical properties.

2. Experimental section

2.1. Materials

The investigated TPU was a Desmopan DP 9370AU (shore hardness = 70A, melt flow index = 35–55 cm^3/10 min), supplied by Bayer (Germany) and consisted of C4 polyether (poly tetramethylene ether glycol) as polyol, butane-diol as chain extender and methylene-diphenyl diisocyanate (MDI) as isocyanate. The OMLS was a Cloisite 30B purchased from Southern Clay Products Inc. (Texas-USA), a natural montmorillonite modified with a quaternary ammonium salt (modifier concentration 90 meq/100 g of clay) and the tallow composition is ca. 65% C18, 30% C16, and 5% C14. The OMLS was dried in a *vacuum* oven at 90° for 12 h prior to use.

2.2. Samples preparation

The OMLS was mixed with TPU in a Haake Rheocord internal mixer at 160 °C (60RPM, 6 min, excluded feeding time) and different nanocomposite matrices with several filler contents (0.1%, 0.5%, 2.0%, 6.0%, 10.0% by weight) were produced. Nanocomposite TPU samples are designated as TPUX where *X* is the weight percentage fraction of OMLS. The nanocomposite TPU was used to prepare 500 μm thick films, by compression moulding with a heated plates hydraulic press (Collin Gmbh, model P 300P, Germany). The mixed TPU was dried in *vacuum* at 90 °C for 12 h, pressed at 10 bar and 180 °C, and then cooled under pressure at 10 °C/min. The specimens cut from films were dried in vacuum at 90 °C for 12 h before testing.

2.3. Dynamic mechanical analysis

Dynamic mechanical tests were carried out by means of a DMA Tritec 2000 (Triton, UK) in tensile deformation. Temperature scan tests were performed applying a tensile amplitude of 10 μm at 1 Hz frequency and at heating rate of 4 °C/min from −120 to 120 °C. Furthermore, strain sweep of the TPU samples was studied at a frequency of 1 Hz and 30 °C, while frequency scan tests were carried out in the range 0.01–40 Hz and at 30 °C. In order to evaluate the effect of SDs crystallization on TPU dynamic mechanical properties, time scan DMA tests were performed in tensile configuration at -10 °C on samples sized 20 mm in length, 5 mm in width and 0.5 mm in thickness.

2.4. Calorimetric analysis

The thermal properties were carried out with a differential scanning calorimeter (DSC 2920, TA Instruments, USA) under N_2 purge in the −70°/+220 °C temperature range. The mass of samples was around 9 mg. The heating scans were performed at a rate of 20 °C/min. Isothermal scan were preformed at −10 °C for 210 min on TPU samples in order to record the crystallization of SDs.

2.5. Small angle X-ray scattering

SAXS analyses were performed by using an Anton Paar SAXSess (Austria) diffractomer (40 kV, 50 mA) equipped with a CuK_α radiation (λ = 0.1542 nm) source and an image plate detector. The tests were carried out at 30 °C. The spectra were collected in transmission mode using the line collimation. The scattering data were dark current,

background and Porod subtracted, normalized for the primary beam intensity and desmeared.

2.6. Fourier transform infra red spectroscopy

FT-IR in ATR mode was used to study the effect of the OMLS on the TPU phase separation. Spectra were collected by using a Nicolet 7199 (Thermo Scientific, Germany) infrared spectrophotometer in the spectral range 400–4000 cm^{-1} with a resolution of 4 cm^{-1}.

3. Results

3.1. Thermal characterization

DSC scan of neat TPU showed an exothermic peak associated to SDs crystallization around −20 °C followed by an endothermic peak due to SDs melting (Fig. 1) as also detected elsewhere [27,28]. Crystallization temperature of SDs did not show any relevant dependence upon OMLS content (Table 1). At higher temperatures an inflection point and an endotherm were detected and labeled T1 and T2, respectively, according to nomenclature adopted by other authors [31,32,42–44]. Generally, T1 is an endothermic peak and has been associated to the interaction between hard and soft segments [44], in particular, to the disordering of non-ideally packed hard segments in the interfacial region between soft and hard phases [32,45,46]. The wide T_2 peak has been related to the ordered/disordered transition of HDs with various degree of organization due to the distribution in hard segment lengths [32,42,44]. The T1 temperature and the extension of the T2 endotherms depend on the thermal history; moreover they can be moved by thermal annealing until merging in a single endotherm peak [32,44].

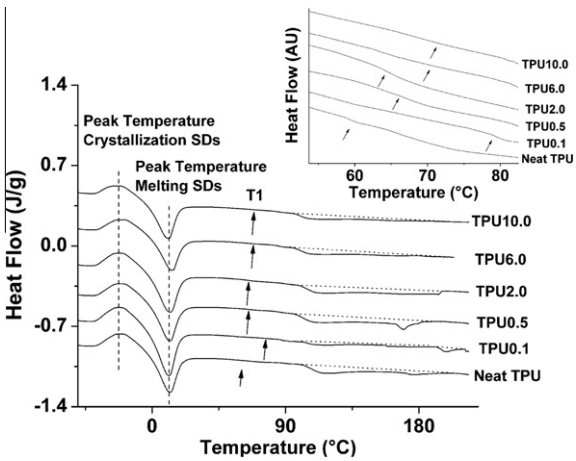

Fig. 1. DSC thermogram of TPU nanocomposites, the curves are shifted for clarity. In the inset the magnification of T1 endotherm zone is reported.

T2 event is a wide endotherm with a first peak around 110 °C and a second one around 160 °C (Fig. 1). The enthalpy associated to the T2 endotherm was measured by considering its value as an estimation of the amount of hard segments organized in HDs.

Layered silicates added into TPU affected the melting enthalpy of SDs, T_g and endotherms. Glass transition of SDs was determined as the temperature of loss tangent peak of DMA curves (being dynamic mechanical analysis more sensitive than DSC in detecting T_g of TPU nanocomposites [25,31,32]). TPU0.1 showed an increase of both T_g and enthalpy of melting of SDs with respect to neat TPU (Table 1 and Fig. 2). The shift towards higher temperature of SDs T_g may be assigned to an increase of hard segments dissolved in SDs [46–49]. Furthermore the melting enthalpy associated to the T2 endotherm was negligible hence the amount of hard segments organized in HDs decreased. The temperature associated to the relaxation T_1 increased indicating a stronger interaction at SD/HD interface or an interface dominated by hard segments thermal properties (Fig. 3).

In sample TPU0.5 the enthalpy of T2 increased and that of SDs was almost unchanged with respect to neat TPU, while SDs T_g achieved the highest value (Fig. 3). In samples TPU2.0, TPU6.0 and TPU10.0 the enthalpy of T2 endotherms decreased with silicate content (Fig. 2). In all samples (but TPU0.1) the increase (or decrease) of enthalpy of the SDs melting corresponded to an increase (or decrease) of T2 endotherms enthalpy respectively, outlining that addition of OMLS into TPU induces a variation in microphases distribution.

The isothermal DSC scan performed at −10 °C provided information on the overall amount of crystallizable SDs. The enthalpy of crystallization of all TPU samples is reported in Table 1 while DSC thermograms of SDs isothermal crystallization are illustrated in Fig. 4. The enthalpy of TPU0.1 sample increased with respect to that of neat

Table 1
Thermal properties of TPU samples.

Clay% wt	Glass transition temperature SDs [°C] peak loss tangent DMA	Melting enthalpy of soft domains [J/g] DSC	T1 DSC [°C]	Enthalpy of T2 endotherm [J/g] DSC	Heat of crystallization soft domains isothermal scan [J/g] DSC	Crystallization temperature of SDs [°C]
0	−55.61	13.11	59.31	9.02	61.31	−19.49
0.1	−54.47	15.69	77.05	1.95	67.88	−20.66
0.5	−52.99	13.76	66.67	11.68	44.64	−19.00
2.0	−54.83	14.35	64.73	12.24	27.95	−19.68
6.0	−54.22	12.44	65.74	7.54	14.44	−19.20
10.0	−56.52	12.57	67.64	7.63	22.13	−21.16
10.0 (quenched)	−56.78	8.24	48.10	6.73	//	//

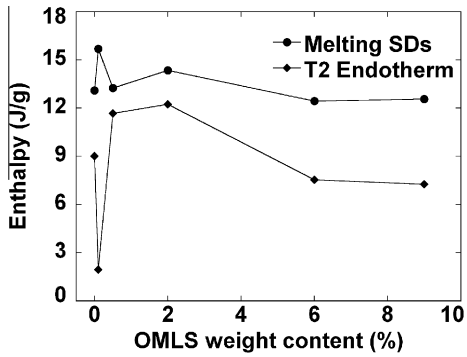

Fig. 2. Melting enthalpy of soft domains and enthalpy of T2 endotherms.

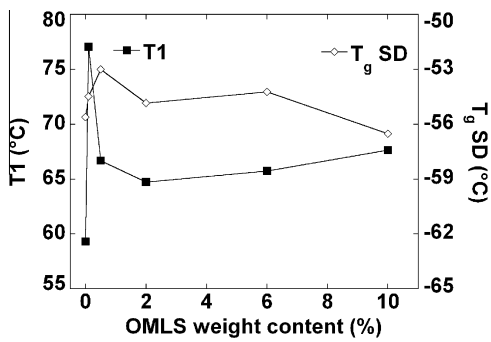

Fig. 3. T1 temperatures (from DSC measurements) and glass transition temperatures of SDs (from DMA measurement), as functions of the OMLS content.

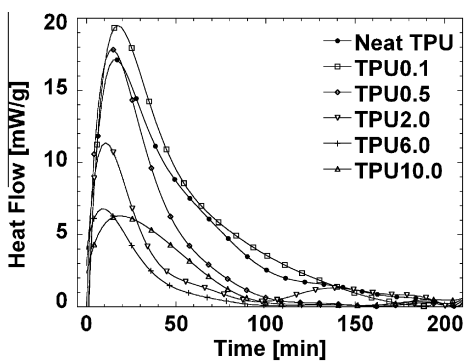

Fig. 4. Heat flow versus time of isothermal DSC experiment at −10 °C.

TPU sample, while decreased in the samples with higher nanofiller contents. These results show that the amount of crystallizable SDs decreases with the OMLS content (except for TPU0.1 sample) and demonstrate that the silicates hinder the crystallization of SDs.

3.2. Morphological investigation

3.2.1. Small angle X-ray scattering analysis

The diffraction pattern of the neat TPU displays a characteristic knee at $q \approx 0.4\ nm^{-1}$ due to the segregation of hard segments to form HDs, whereas the diffraction pattern of TPU10.0 shows an additional peak at $q = 1.6\ nm^{-1}$ ascribed to the OMLS (0 0 1) peak (Fig. 5A). Since the pristine OMLS exhibits a diffraction peak at $q = 3.26\ nm^{-1}$ corresponding to the inter-platelets distances of $d_{0\,0\,1} = 1.9$ nm (inlet graph of Fig. 5B), the shift of (0 0 1) peak at $1.6\ nm^{-1}$ in the TPU2.0, TPU6.0 and TPU10.0 diffraction patterns highlights an increase on the inter-platelets distance up to $d_{0\,0\,1}$ of 3.9 nm (Fig. 5B). This value clearly indicates that macromolecule chains have intercalated into the galleries of the OMLS. However no peaks were observed for samples TPU0.1 and TPU0.5. This might be due to the presence of OMLS partially or completely exfoliated.

In order to have a better understanding of TPU structure through SAXS analysis it has been necessary to isolate the TPU diffraction features from the nanocomposites scattering by subtracting the OMLS contribute. Vaia et al. [50] found that layered silicates exhibit at q values lower than the OMLS (0 0 1) peak a power-law dependence as $I(q) = Aq^m$, where the m exponent is -2 or less, for silicate stacks, decreasing with increasing stack size. Therefore the theoretical scattering intensity $I(q)_{OMLS} = Aq^m$ ascribed to the OMLS was subtracted from the nanocomposites scattering profiles $I(q)_{Nanoc}$, by selecting the m value equal to -2. The pre-exponential factor A was calculated making equal the $I(q)$, resulting from subtraction, which represents the scattering intensity of TPU inside the nanocomposites, to the scattering intensity of neat TPU at $q = 0.11\ nm^{-1}$. The resulting Lorentz corrected SAXS patterns of the TPU matrix in the several nanocomposites are shown in Fig. 5C.

Since the analysis of the curve relative to the neat TPU sample at small q (Fig. 5A) provided a slope value close to zero, the HDs have been regarded as arranged in a globular morphology [50]. Additionally, the average distance d between HDs has been evaluated by means of the Bragg's equation taking into account the scattering vector at maximum intensity of TPU peak [3,21,31,51]. The interdomain distance between the HDs in the TPU nanocomposites is reported in Table 2. The addition of OMLS did not affect significantly the interdomain distance (the value provided by SAXS analysis is the mean value of a distribution of interdomain distance). In fact, the mean distance between HDs increased from 14.76 (for neat TPU) to 16.10 nm (for TPU10.0). However, it is worth noting that the peak in Iq^2 vs q plot broadens with increasing OMLS content (Fig. 5C). This broadening has been quantified through the calculation of the polydispersivity, defined as $M^* = q_0/q_{max}$, where q_{max} and q_0 (see Fig. 5C) are the q value corresponding to the peak and the intercept on the q axis of the tangent at the inflection point, respectively [53,54]. The results show that the polydispersivity, indicative of the interdomain distances distribution around the mean value, increases with the filler amount (Table 2). Addition of OMLSs influences the formation and segregation mechanism of HDs, resulting in structures with enlarged distribution of interdomain distances.

3.2.2. Phase separation degree by FT-IR spectroscopy

The degree of phase separation (DPS) between hard and soft domains can be evaluated by estimating the amount of carbonyl groups involved in hydrogen bonding with the

amide in urethane group. The higher the amount of hydrogen bonded carbonyl groups, the higher the DPS [20]. Since the peak at 1732 cm^{-1} is attributed to the free-of-hydrogen-bonding carbonyl and the peak at 1702 cm^{-1} is associated with the hydrogen-bonded carbonyl, it is possible to evaluate the hydrogen bonding degree by measuring the peak intensity ratio of these two carbonyl groups. The carbonyl hydrogen bonding index, *R*, is:

$$R = \frac{C_{bonded}\varepsilon_{bonded}}{C_{free}\varepsilon_{free}} = \frac{A_{1702}}{A_{1732}}$$

where *A* is the intensity of the characteristic absorbance, C_{bonded} and C_{free} are the concentrations and ε_{bonded} and ε_{free} are the extinction coefficients of the bonded and free carbonyl groups, respectively.

In the hypothesis that $\varepsilon_{bonded}/\varepsilon_{free} = 1$ in TPU [20], the index *R* represents the concentrations ratio between hydrogen-bonded and free-of-hydrogen-bonding carbonyls. Hence the DPS can be calculated as follows [20,21,55]:

$$DPS = \frac{C_{bonded}}{C_{bonded} + C_{free}} = \frac{R}{R+1}$$

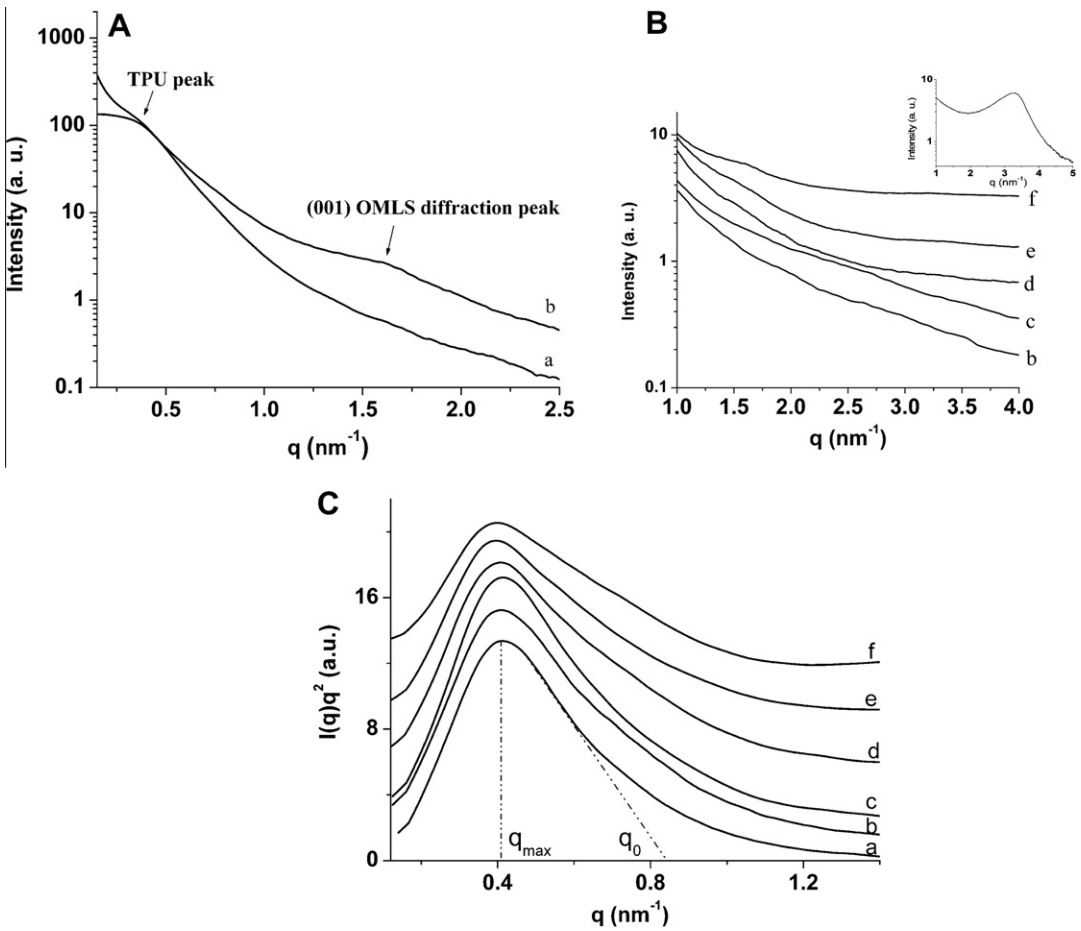

Fig. 5. (A) Diffracted intensity of neat TPU (a) and TPU10.0 (b). (B) Diffracted intensity of TPU0.1 (b), TPU0.5 (c), TPU2.0 (d), TPU6.0 (e), TPU10.0 (f) and pristine OMLS in the inset graph. (C) The Lorentz-corrected plots of Neat TPU (a); TPU0.1 (b); TPU0.5 (c); TPU2.0 (d); TPU6.0 (e); TPU10.0 (f) nanocomposites after subtraction of OMLS scattering intensity. The curves have been vertically shifted for clarity.

Table 2
Morphological data obtained from SAXS and FT-IR analyses.

Sample	Interdomain distance [nm]	Polydispersivity	Degree of phase separation
Neat TPU	14.76	2.00	0.52
TPU0.1	15.90	2.38	0.51
TPU0.5	14.95	2.26	0.49
TPU2.0	15.47	2.46	0.59
TPU6.0	15.77	2.58	0.58
TPU10.0	16.10	2.80	0.60
TPU10.0 quenched			0.55

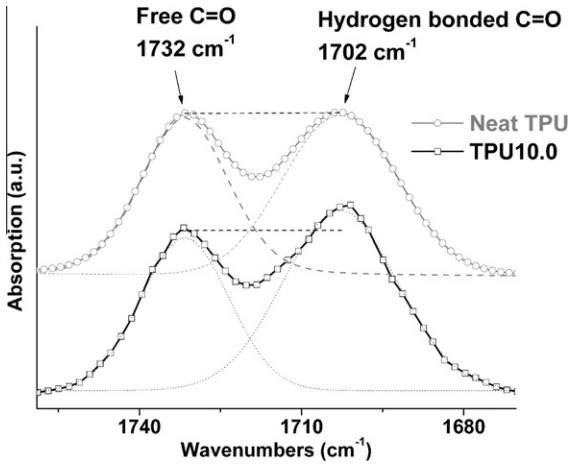

Fig. 6. FT-IR spectra in the carbonyl absorbance bands for TPU and TPU10.0 deconvoluted by software elaboration.

In order to measure the area of the absorbance peaks at 1702 and 1732 cm^{-1}, a software deconvolution process of the spectral region of the carbonyl groups (i.e. 1660–1750 cm^{-1}) has been carried out. In particular, a Gaussian function has been used to fit the single absorbance peak. The deconvolution of the samples neat TPU and TPU10.0 are shown in Fig. 6 and the DPS values of all TPU samples are reported in Table 2. The DPS of the samples TPU0.1 and TPU0.5 decreased, while it increased at higher OMLS content with respect to that of neat TPU, hence the addition of OMLS into TPU resulted in a modification of microphase segregation.

3.3. Viscoelastic properties

3.3.1. Effect of temperature

The dynamic mechanical analyses of the TPU samples in −120/+120 °C temperature range showed an increase of the storage modulus with the OMLS content (Fig. 7A). Such an increase is more evident upon melting of SDs, as detected also elsewhere [27,29]. In the temperature range −50/+20 °C, the storage modulus curve of all samples present a shoulder due to SDs crystallization, clearly detected in DSC thermograms as well. The loss tangent value at SDs glass transition temperature decreased with the silicate content due to reduced mobility of macromolecules (Fig. 7B). Samples TPU0.1 and TPU2.0 presented a shift of the loss tangent peaks towards higher temperatures testifying the presence of hard segments in SDs, as already mentioned the results of DSC measurements [46–49]. The loss tangent curves exhibited a shoulder in correspondence of the SDs crystallization pattern. The variation of loss tangent due to crystallization is discussed in more detail below.

In the temperature ranges between 10 and 120 °C the loss tangent of the samples TPU6.0 and TPU10.0 increased with respect to neat TPU. This trend has been also detected in either DMA strain scan tests at low strain (linear viscoelastic region), performed at 30 °C and 1 Hz (Fig. 8B), or DMA frequency scan test carried out at 30 °C (Fig. 10C).

3.3.2. Effect of strain

The results of dynamic strain scan analyses have shown that the storage modulus of nanocomposite TPU samples increased with OMLS loadings. At low strain, the storage modulus of TPU samples increases with the silicate content (Fig. 8). The storage modulus of the sample TPU10.0 is about sixfold higher than that of neat TPU at low strain. As dynamic strain increases, the storage modulus of neat TPU and nanocomposite TPU samples with low filler content is constant up to 2% of amplitude. The samples TPU6.0 and TPU10.0 show an evident non linear behavior characterized by the storage modulus reduction as dynamic strain value exceeds 0.1% (0.2% for TPU6.0 sample). This dynamic behavior is dominated by the Payne effect [41], as already reported in other papers on TPU filled with OMLS [27] and carbon nanofiber [40].

The loss tangent of samples containing low amount of silicates (0.1–2% wt) was quite similar to neat TPU and slightly increased at higher strains (Fig. 8B). Conversely, samples TPU6.0 and TPU10.0 exhibited higher loss tangent than neat TPU at low strains, and a stronger dependence upon deformation. The silicate addition into TPU reduced the linear viscoelastic strain range of one order of magnitude, from 2% for the neat TPU to 0.1% for TPU10.0.

In order to investigate the influence of phase segregation on viscoelastic properties of TPU, strain scan tests were performed also on TPU10.0 sample obtained by quenching during the cooling stage of the compression

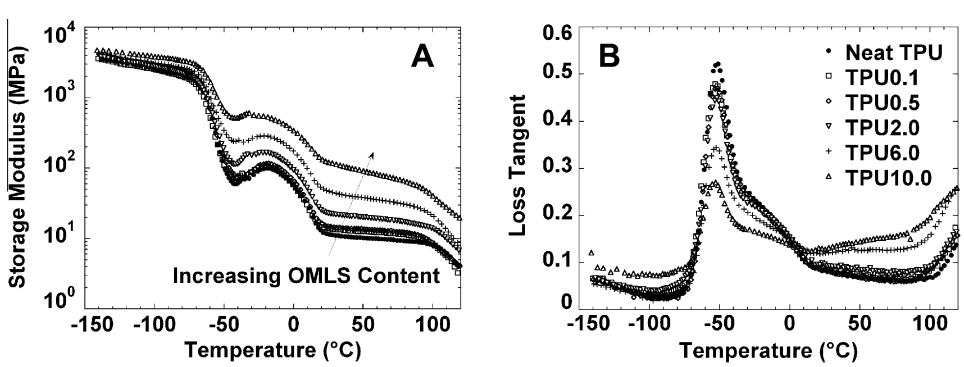

Fig. 7. Temperature scan test of TPU samples: (A) Storage modulus and (B) loss tangent.

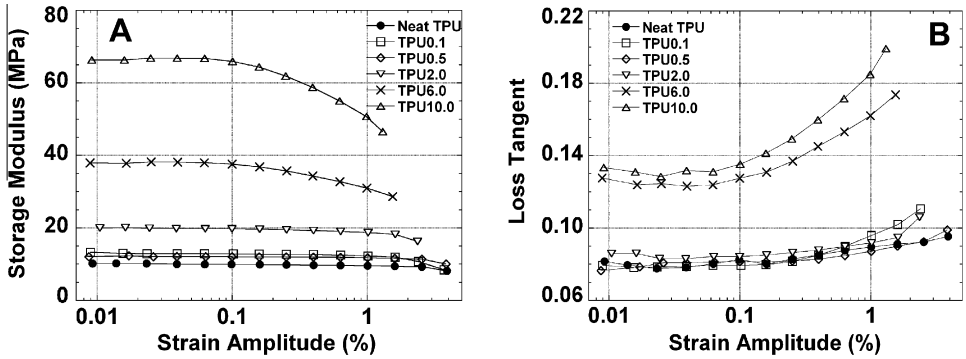

Fig. 8. Strain scan test of TPU samples at 30 °C: (A) Tensile storage modulus and (B) loss tangent.

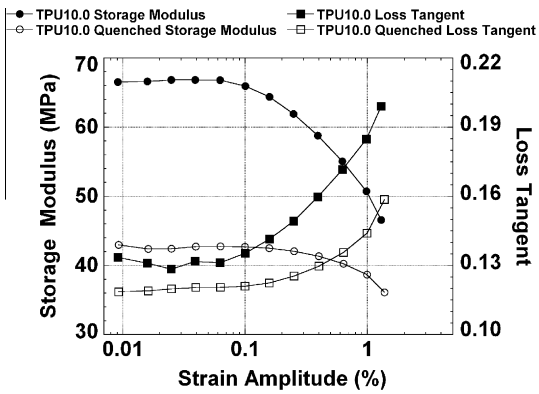

Fig. 9. Tensile storage modulus and loss tangent of samples TPU10.0 and quenched-TPU10.0 as function of strain amplitude.

moulding process (cooling rate = 50 °C/min). The quenched TPU10.0 sample showed a decrease of both storage modulus and loss tangent with respect to the not-quenched TPU10.0 sample and a wider linear viscoelastic strain region (Fig. 9). The DSC analysis of this sample illustrated a decrease of both the melting enthalpy of SDs and the T1 temperature (Table 1). While the DPS increased with respect to not-quenched TPU10.0 (Table 2). These results suggest the formation of an HDs/SDs interface, probably characterized by a diffuse boundary [2–4], made up predominantly by soft segments. Consequently the total amount of elastomeric SDs reduced due to lower availability of soft segments. The different behavior of quenched and not-quenched TPU10.0 samples evidenced a dependence of viscoelastic behavior of filled TPU on the microdomain morphology. In particular, the decrease of the enthalpy of melting of SDs resulted in a reduction of elastomeric phase (SDs) that leads to lower viscoelastic properties (storage modulus and loss tangent), in addition to a less pronounced non linear behavior (Payne effect).

3.3.3. Effect of frequency

All the samples were tested applying a tensile amplitude displacement of 10 μm (0.1% strain) unless TPU6.0 and TPU10.0 samples whose amplitude displacement was set 5 and 2 μm, respectively, in order to evaluate the frequency response (0.01–40.0 Hz) in the linear viscoelastic strain range (see Fig. 8). The storage modulus and loss moduli of TPU samples increased with frequency in all compositions and they increased also with silicate content (Fig. 10A and B). The slope of moduli became steeper with increasing filler loadings. The loss tangent increased with increasing silicate content at low frequencies but all curve converged at high frequencies. The convergence is probably due to resonance of the material which prevented the instrument a correct data analysis collection [27].

3.3.4. Effect of SDs crystallization

The storage modulus of the TPU samples increased with elapsing time and reached a plateau value (Fig. 11A). The modulus enhancement indicated that crystallization took place and that the crystallites were able to reinforce TPU [56]. It is likely that crystallites were forming in the core of SDs, where the soft segments should have higher mobility than those at interface with HDs. An illustration of crystallites formation, based on both morphological analysis results and several models proposed for the TPU microdomains [15,39,46,52] has been suggested (Fig. 12). In the plateau region, the storage modulus of the nanocomposites increased monotonically with silicate content. The loss modulus of nanocomposites presented a trend similar to that of storage modulus (Fig. 11B); conversely, the loss tangent of nanocomposite TPU samples showed a different behavior (Fig. 11C). The loss tangent of samples neat TPU, TPU0.5, TPU2.0 and TPU6.0 increased with the crystallization process till a maximum value occurring after 100, 70, 55 and 30 min, respectively, and then decreased with the increasing OMLS content. Loss tangent of sample TPU0.1 presented an evident plateau at long times and the highest loss tangent value in the plateau region; while that of sample TPU10.0 did not evidence any maximum value. The maximum loss tangent values can be evidently ascribed to the crystallization. In fact, while crystalline phases increase, the thickness of the SDs layers, included between crystallized SDs and HDs, decreases. The loss tangent maximum (in each nanocomposites TPU) corresponds to the layer thickness (Fig. 12) that maximize the dissipative phenomena. The absence of a maximum value for the sample TPU0.1 is seemingly related to the longer SDs mean size (note that the enthalpy of melting of SDs of this sample

is the highest) that caused the maximum to occur in timeframe higher than 200 min. Instead, lack of a peak value of loss tangent for TPU10.0 could be due to: (a) a crystallization rate higher than that of the other samples, that induced the peak value to be reached before the data acquisition during the isothermal DMA scan (the environmental chamber took about 2 min to reach −10 °C); (b) the loss tangent of TPU10.0 decreased during crystallization because the microdomain morphology already maximized dissipative phenomena (note that the loss tangent values of both TPU6.0 and TPU10.0 samples were higher than that of the other sample at the early stages of the isothermal scan test).

4. Discussion

In our experiments, even though the HDs interdomain distance did not show any significant variation with OMLS content (Table 2), silicates have influenced both microphase segregation (DPS) and distribution of the interdomain distance (polydispersivity), and consequently have had a significant influence on both thermal and dynamic mechanical properties of the TPU nanocomposites. In order to further comprehend these aspects, the specific surface area of both HDs and OMLS stacks/platelets into the TPU systems has been estimated. As already mentioned, the analysis of the slope value of the neat TPU at low q has suggested that the HDs had globular shape. Therefore, in order to calculate the specific surface area, the structure of the HDs into TPU has been considered as a three-dimensional ordered array of spheres with mean distance of 14.76 nm (Table 2). In addition, the specific surface area of OMLS stacks was calculated assuming their shape as flat discs with variable thickness and diameter. The specific surface area of silicate discs with variable diameter length (100, 200 and 500 nm) as function of the degree of exfoliation/intercalation (i.e. silicate stacks thickness) is illustrated in Fig. 13. The disk diameter has been included in the typical range of the length of the OMLS platelets/stacks (Cloisite 30B) incorporated in the TPU, as detected in several papers [25,27,30–33]. The gray zone (Fig. 13) represents the specific surface area of spherical HDs with mean diameters ranging from 2.5 (lower limit) to 3.5 nm (upper limit) [15,39]. Noteworthy is that the specific surface area was evaluated assuming the diameters of both HDs and platelets disc monodisperse, hence they only provide an estimation of the order of magnitude. It is evident that, starting from an OMLS content of 2%, the specific surface area of dispersed filler becomes comparable with that of HDs, indeed the extents of the interfaces HDs/SDs and OMLS/SDs become of the same order of magnitude.

Investigation of the relationships SDs T_gs-versus-DPS (Fig. 13) and T1-versus-polydispersivity (Fig. 14) has permitted to better understand the influence of the OMLS on both microdomain morphology and interfaces into the TPU (HDs/SDs, OMLSc/SDs).

A decrease of DPS (an estimation of segregation of the hard and soft domains) results in hard segments dissolved in SDs (in the hypothesis that soft segments do not dissolve in HDs and that all carbonyls in HDs are bonded [57]). Such a phenomenon is responsible for the increase in SDs T_gs, as already mentioned [46–49]. Two groups of data with a decreasing trend are evident in the plot of Fig. 14: the first one contains samples with OMLS less then 2%, while the second one, at higher DPS values, includes the samples TPU2.0, TPU6.0 and TPU10.0. As expected, within these groups the T_g of the SDs decreases with the increasing DPS. The influence of OMLS on the mechanism of the TPU morphology formation clearly changes when it reaches a concentration of 2.0% that is the concentration at which the specific surface area of the filler becomes comparable with that of HDs.

The polydispersivity calculated by means of SAXS measurements provides an indirect estimation of the interface extent between HDs and SDs. In fact, it represents the distribution of the separation distance between HDs around a mean value; when this distribution broadens towards higher q values it describes a morphology characterized by shorter interdomain distance [53,54,58]. However, if the interdomain distance decreases and the HDs amount is unchanged, their size should decreases (otherwise the HDs would be in contact [39,58]). In such conditions, the addition of OMLS into TPU leads to a microdomain morphology characterized by a higher extent of interface between HDs and SDs. The increase of HDs interface area with the increasing polydispersivity is confirmed by the T1-vs-polydispersivity plot (Fig. 15), in which, also in these case, two groups of data can be distinguished. The first one includes samples neat TPU, TPU0.1 and TPU0.5, while the second one is described by the samples containing an OMLS concentration in excess of 0.5%. In fact T1 event was attributed to the interaction between hard and soft segments [32,44,45], indeed it depends on the properties and/or extent of the interface between HDs and SDs. Hence, the growth of T1 as function of the increasing polydispersivity, within the two groups, verifies the relationship between polydispersivity and interface extent between HDs and SDs.

The discontinuity, detectable in both plots of Figs. 14 and 15, is due to a change of microdomain morphology in the TPU samples. In particular, it occurs at 2% OMLS content when the extent of the OMLSs/SDs interface approaches that of the HDs/SDs interface (note that the OMLSs/HDs interface was considered negligible). Nevertheless, starting from 2% wt concentration, the OMLS stacks still influence the microdomain morphology formation as demonstrated by the modification of both DPS and polydispersivity.

In a plot of the storage modulus and loss tangent of TPU samples (taken from strain scan test in the linear viscoelastic region) versus polydispersivity, two increasing trends with variable slope can be detected (Fig. 16). Even in this case a discontinuity of the trends occurs at 2.0% wt content of OMLS. The viscoelastic properties in filled elastomeric matrix are determined by the polymer/filler interface, in particular higher interface extent results in higher storage modulus as well as loss modulus [59]. In our systems, the addition of OMLS resulted in the increase of both storage and loss modulus in all TPU nanocomposites. Strain scan test showed a more pronounced non-linear behavior at higher OMLS content, as detected in other works on TPU

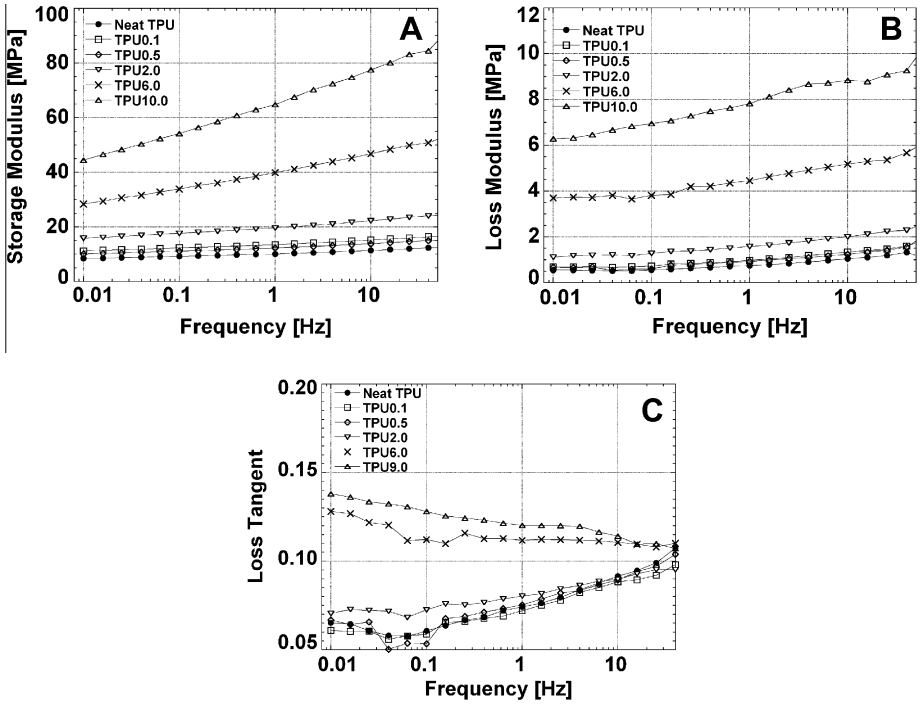

Fig. 10. Frequency scan test at 30 °C of TPU samples: (A) storage modulus, (B) loss modulus and (C) loss tangent.

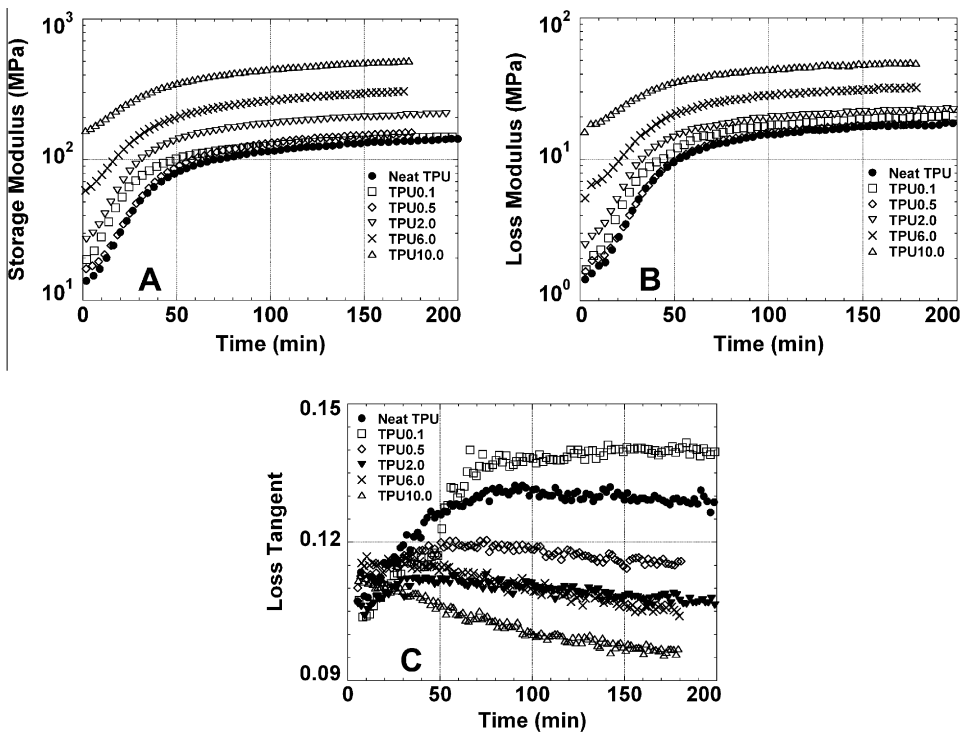

Fig. 11. Isothermal DMA test at −10 °C and 1 Hz on TPU samples: (A) storage modulus; (B) loss modulus and (C) loss tangent.

filled with OMLSs [27], carbon nanofibers [40] and elastomeric matrix filled with spherical nanoparticles [59,60]. The increase of HDs/SDs interface (i.e. polydispersivity) in the TPU systems, induced by the OMLS at low filler

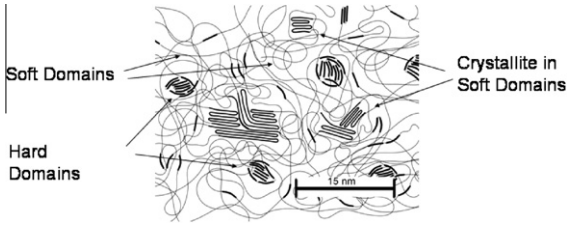

Fig. 12. Schematic representation of SDs crystallization in neat TPU.

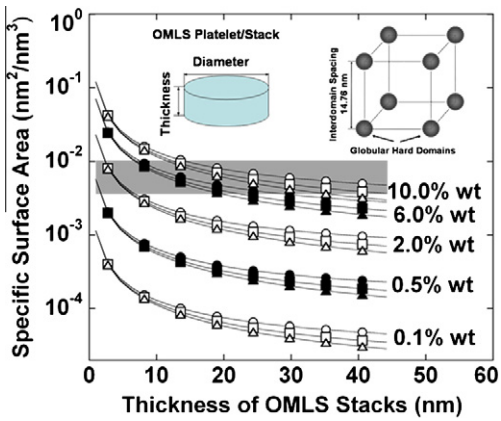

Fig. 13. Specific surface area of discoid OMLS stacks with variable diameter length (circle = 100 nm, square = 200 nm, triangle = 500 nm) as function of both stack thickness and concentration into TPU samples. The gray rectangle represents the specific surface area of spherical HDs with diameter ranging between 2.5 (lower limit) and 3.5 nm (upper limit).

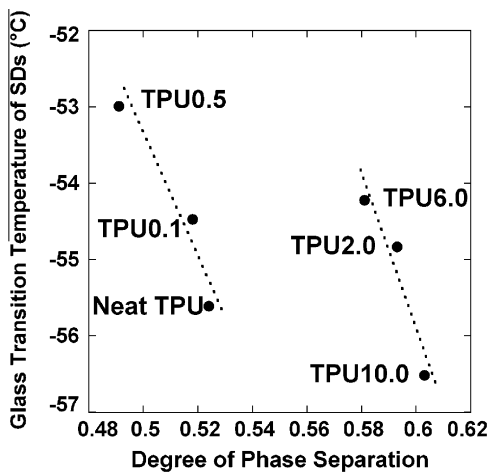

Fig. 14. Glass transition temperature of SDs as function of degree of phase separation in TPU samples.

content, results in a loss tangent increment (Fig. 16). Note that both storage modulus and loss tangent of sample TPU0.1 (Fig. 16) are higher than those of sample TPU0.5 (with lower polydispersivity), evidencing an order relationship of both storage modulus and loss tangent with polydispersivity. At filler contents higher than 2%, the

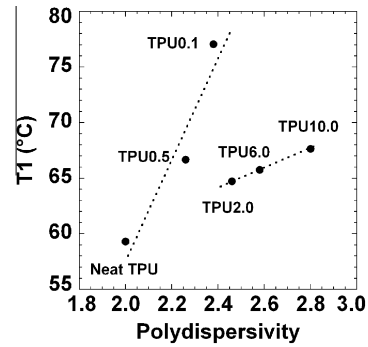

Fig. 15. T1 temperature as function of polydispersivity of TPU samples.

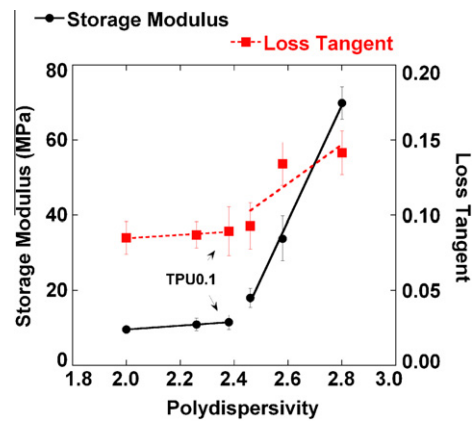

Fig. 16. Storage modulus and loss tangent of TPU samples as function of the polydispersivity.

slopes of both storage modulus and loss tangent become steeper showing that, in addition to the OMLS effect on modification of the microdomain morphology (polydispersivity), the OMLS stacks contribute to create an additional interface with SDs, boosting the properties enhancement governed by the increase of the SDs interfaces. It is worth to point out that the reinforcing effect of the filler is lower in case of reduced interface between SDs and OMLS stacks/platelets, as demonstrated by dynamic mechanical properties of the quenched-TPU10.0 sample. This sample has shown the lowest amount of SDs enthalpy of melting (Table 1) and a very low DPS (Table 2), indicating a reduction of the overall elastomeric phase (SDs) as well as a decrease of the extent of OMLS/SDs interface. Such a decrease is responsible for the lower reinforcement of OMLS stacks/platelets into quenched TPU10.0 with respect to OMLS dispersed into the not-quenched-TPU10.0 sample. A further prove of the fundamental role of SDs interface on the viscoelastic properties of TPU system is provided by the analysis of isothermal DMA experiments (Fig. 11). In fact, during crystallization of SDs, crystalline domains form within the "core" of SDs creating new interfaces between crystallized and not-crystallized SDs. The generation of these interfaces results in setting up of new trapped entanglements that leads to increase of both storage and loss moduli [59].

The influence of OMLS on the microdomain morphology is quite complex, we propose a mechanism based on the interactions of both hard and soft segments with OMLS surface. In fact the latter is formed by either hydrophilic or hydrophobic regions that could arrange together the hydrophilic hard segments and hydrophobic soft segments, acting as template [35] and forcing a local mixing of hard and soft segments that results in a decrease of DPS at low loadings (Table 2). The typical stack size of the OMLS (30B SouthernClay) dispersed in TPU varies from 100 to 500 nm [25,27,30–33], definitively longer than the scale of the investigated microdomain morphology. Therefore the OMLS stacks cannot be located preferentially in one of the two phases but the local arrangements at stacks/macromolecules interface result in far-field constrains that modify microdomain morphology. At higher OMLS contents, when interaction among stacks/platelets is not negligible, the microdomain morphology is also influenced by geometrical constrains.

Summarizing, the OMLS contributes to the modification of TPU microdomain morphology, leading to an increase of interfaces between HDs and SDs. Furthermore silicate platelets form additional interfaces with SDs, for concentrations equal to or higher than 2%. These two processes affect the TPU microdomain morphology as well as its viscoelastic and thermal properties.

5. Conclusions

Thermal and dynamic mechanical properties of nanocomposites TPU samples based on OMLS and prepared by melt blending have shown a clear dependence upon silicate content. FT-IR spectroscopy has illustrated that the microphase segregation of the TPU decreases at low OMLS content (0.1 and 0.5% wt) evidencing a compatibilizing effect of the silicates. At higher OMLS concentrations, on the other hand, an increase of microphase segregation was detected. SAXS measurements have demonstrated that the distribution of HDs interdomain distance broadens with increasing filler content and consequently, the extent of the HDs/SDs interface increases.

Analysis of the relationships between microdomain morphology (DPS, polydispersivity) and dynamic–mechanical/thermal properties has clearly indicated that the influence of OMLS on the formation mechanism of the TPU morphology changes at 2% content. This analysis has also shown that the properties of the TPU nanocomposite are mostly governed by the extent of the SDs interface with both OMLS stacks/platelets and HDs. In particular, the investigation of both effects of quenching on TPU samples and variation of viscoelastic properties during crystallization of SDs, has demonstrated that increase of the interface area of the elastomeric SDs results in enhancement of storage modulus and loss tangent in the TPU.

References

[1] Drobny JG. Handbook of thermoplastic elastomers. Norwich, NY: William Andrew Publishing; 2007 (Chapter 9).

[2] Garrett JT, Runt J, Li JS. Microphase separation of segmented poly(urethane urea) block copolymers. Macromolecules 2000;33:6353–9.

[3] Leung LM, Koberstein JT. Small-angle scattering analysis of hard-microdomain structure and microphase mixing in polyurethane elastomers. J Polym Sci Pol Phys 1985;23:1883–913.

[4] Bonart R, Müller EH. Phase separation in urethane elastomers as judged by low-angle X-ray scattering. I. Fundamentals. J Macromol Sci Phys Ed 1974;B10:177–89.

[5] Cooper SL, Tobolsky AV. Properties of linear elastomeric polyurethanes. J Appl Polym Sci 1966;10:1837–44.

[6] Koberstein JT, Russell TP. Simultaneous SAXS-DSC study of multiple endothermic behavior in polyether-based polyurethane block copolymers. Macromolecules 1986;19:714–20.

[7] Bonart R. X-ray investigations concerning the physical structure of crosslinking in segmented elastomers. J Macromol Sci 1968;B2:115–38.

[8] Bonart R, Morbitzer L, Hentze GJ. X-ray investigations concerning the physical structure of crosslinking in segmented elastomers II Butanediol as chain extender. Macromol Sci 1969;B3:337–56.

[9] Bonart R, Morbitzer L, Müller EH. X-ray investigations concerning the physical structure of crosslinking in urethane elastomers. III. Common structure principles for extensions with aliphatic diamines and diols. J Macromol Sci 1974;B9:447–52.

[10] Wilkes CW, Yusek C. Investigation of domain structure in urethan elastomers by X-ray and thermal methods. J Macromol Sci 1973;B7:157–75.

[11] Clough SB, Schneider NS. Structural studies on urethane elastomers. J Macromol Sci 1968;B2:553–66.

[12] Clough SB, Schneider NS, King AO. Small-angle X-ray scattering from polyurethane elastomers. J Macromol Sci 1968;B2:641–8.

[13] Blackwell J, Nagarajan MR. Conformational analysis of poly(MDI-butandiol) hard segment in polyurethane elastomers. Polymer 1981;22:202–8.

[14] Huh DS, Cooper SL. Dynamic mechanical properties of polyurethane block polymers. Polym Eng Sci 1971;11:369–76.

[15] Koerner H, Kelley JJ, Vaia RA. Transient microstructure of low hard segment thermoplastic polyurethane under uniaxial deformation. Macromolecules 2008;41:4709–16.

[16] Garrett JT, Siedlecki CA, Runt J. Microdomain morphology of poly(urethane urea) multiblock copolymers. Macromolecules 2001;34:7066–70.

[17] McLean RS, Sauer BB. Tapping-Mode AFM studies using phase detection for resolution of nanophases in segmented polyurethanes and other block copolymers. Macromolecules 1997;30:8314–7.

[18] O'Sickey MJ, Lawrey BD, Wilkes GL. Structure-property relationships of poly(urethane urea)s with ultra-low monol content poly(propylene glycol) soft segments. I. Influence of soft segment molecular weight and hard segment content. J Appl Polym Sci 2002;84:229–43.

[19] Aneja A, Wilkes GL. A systematic series of 'model' PTMO based segmented polyurethanes reinvestigated using atomic force microscopy. Polymer 2003;44:7221–8.

[20] Tien TI, Wei KH. Hydrogen bonding and mechanical properties in segmented montmorillonite/polyurethane nanocomposites of different hard segment ratios. Polymer 2001;42:3213–21.

[21] Seymour RW, Estes GM, Cooper SL. Infrared studies of segmented polyurethan elastomers. i. hydrogen bonding. Macromolecules 1970;3:579–83.

[22] Song M, Xia HS, Yao KJ, Hourston DJ. A study on phase morphology and surface properties of polyurethane/organoclay nanocomposite. Eur Polym J 2005;41:259–66.

[23] Xia H, Shaw SJ, Song M. Relationship between mechanical properties and exfoliation degree of clay in polyurethane nanocomposites. Polym Int 2005;54:1392–400.

[24] Jin J, Song M, Yao KJ, Chen L. A study on viscoelasticity of polyurethane -organoclay nanocomposites. J Appl Polym Sci 2006;99:3677–83.

[25] Pattanayak A, Jana SC. Properties of bulk-polymerized thermoplastic polyurethane nanocomposites. Polymer 2005;46:3394–406.

[26] Chen T, Zhou S, Yang H, Wu L. Structure and properties of polyurethane/nanosilica composites. J Appl Polym Sci 2005;95:1032–9.

[27] Barick AK, Tripathy DK. Effect of organoclay on thermal and dynamic mechanical properties of novel thermoplastic polyurethane nanocomposites prepared by melt intercalation technique. Polym Adv Technol 2010;21(12):835–47.

[28] Barick AK, Tripathy DK. Preparation and characterization of thermoplastic polyurethane/organoclay nanocomposites by melt intercalation technique: Effect of nanoclay on morphology, mechanical, thermal, and rheological properties. Polym J Appl Polym Sci 2010;117:639–54.

[29] Barick AK, Tripathy DK. Effect of organoclay on the morphology, mechanical, thermal, and rheological properties of organophilic montmorillonite nanoclay based thermoplastic polyurethane nanocomposites prepared by melt blending. Polym Eng Sci 2009;50(3):484–98.
[30] Chavarria F, Paul DR. Effect of organoclay on the morphology, mechanical, thermal, and rheological properties of organophilic montmorillonite nanoclay based thermoplastic polyurethane nanocomposites prepared by melt blending. Polymer 2006;47: 7760–73.
[31] Finnigan B, Martin D, Halley P, Truss R, Campbell K. Effect of the Average Soft-Segment Length on the Morphology and Properties of Segmented Polyurethane Nanocomposites. J Appl Polym Sci 2005;97:300–9.
[32] Finnigan B, Martin D, Halley P, Truss R, Campbell K. Morphology and properties of thermoplastic polyurethane nanocomposites incorporating hydrophilic layered silicates. Polymer 2004;45: 2249–60.
[33] Dan CH, Lee MH, Kim YD, Min BH, Kim JH. Exploring preferential association of laponite and cloisite with soft and hard segments in TPU-clay nanocomposite prepared by solution mixing technique. Polymer 2006;47:6718–30.
[34] Mishra AK, Nando G, Chattopadhyay G. J Polym Sci Pol Phys 2008;46:2341–54.
[35] Buffa F, Abraham GA, Grady BP, Resasco D. Effect of nanotube functionalization on the properties of single-walled carbon nanotube/polyurethane composites. J Polym Sci Pol Phys 2007;45:490–501.
[36] Liff SM, Kumar N, Mc Kinley GH. High-performance elastomeric nanocomposites via solvent-exchange processing. Nat Mater 2007;6:76–83.
[37] Chang J-H, An YU. Nanocomposites of polyurethane with various organoclays: Thermomechanical properties, morphology, and gas permeability. J Polym Sci Pol Phys 2002;40:670–7.
[38] Hasegawa N, Usuki A. Arranged microdomain structure induced by clay silicate layers in block copolymer-clay nanocomposites. Polym Bull 2003;51:77–83.
[39] Finnigan B, Jack K, Campbell K, Halley P, Truss R, Casey P, et al. Segmented polyurethane nanocomposites: impact of controlled particle size nanofillers on the morphological response to uniaxial deformation. Macromolecules 2005;38:7386–96.
[40] Schaefer DW, Zhao J, Dowty H, Alexander M, Orler EB. Carbon nanofibre reinforcement of soft materials. Soft Matter 2008;4: 2071–9.
[41] Payne AR. The dynamic properties of carbon black-loaded natural rubber vulcanizates. Part I. J Appl Polym Sci 1962;6:57–63.
[42] Martin DJ, Meijs GF, Gunatillake PA, McCarthy SJ, Renwick GM. The effect of average soft segment length on morphology and properties of a series of polyurethane elastomers. II. SAXS-DSC annealing study. J Appl Polym Sci 1997;64:803–17.
[43] Leung LM, Koberstein JT. DSC annealing study of microphase separation and multiple endothermic behavior in polyether-based polyurethane block copolymers. Macromolecules 1986;19:706–13.
[44] Seymour RW, Cooper SL. Thermal analysis of polyurethane block polymers. Macromolecules 1973;6:48–53.
[45] Eisenbach CD, Baumgartner M, Gunter C. In: Lal J, Mark JE, editors. Advances in elastomers and rubber elasticity. New York: Plenum Press; 1986. p. 51.
[46] Martin DL, Meijs GF, Renwick GM, McCarthy SJ, Gunatillake PA. The effect of average soft segment length on morphology and properties of a series of polyurethane elastomers. I. Characterization of the series. J Appl Polym Sci 1996;62:1377–86.
[47] Chen TK, Chui JY, Shieh TS. Glass transition behaviors of a polyurethane hard segment based on 4,4'-diisocyanatodiphenylmethane and 1,4-butanediol and the calculation of microdomain composition. Macromolecules 1997;30:5068–74.
[48] Duo Y, Tan H, Chen F. Synthesis and characterization of thermoplastic polyurethanes as binder for novel thermoplastic propellant. J Appl Polym Sci 2002;83:2961–6.
[49] Sung CSP, Schneider NS. Infrared studies of hydrogen bonding in toluene diisocyanate based polyurethanes. Macromolecules 1975;8(1):68–73.
[50] Vaia RA, Liu W, Koerner H. Analysis of small-angle scattering of suspensions of organically modified montmorillonite: Implications to phase behavior of polymer nanocomposites. J Polym Sci Pol Phys 2003;41:3214–36.
[51] Guinier A, Fournet G. Small angle scattering of X-rays. New York: John Wiley and Sons; 1955.
[52] Saiani A, Rochas C, Eeckhaut G, Daunch WA, Leenslag JW, Higgins JS. Origin of multiple melting endotherms in a high hard block content polyurethane. 2. structural investigation. Macromolecules 2004;37: 1411–21.
[53] Hosemann R, Bagchi SN. Direct analysis of diffraction by matter. Amsterdam: North Holland Publishing Company; 1962 (chapters 5, 7).
[54] Greco R, Musto P, Riva F. Bulk functionalization of ethylene - propylene copolymers. III. Structural and superreticular order investigations. J Appl Polym Sci 1989;37:789–801.
[55] Pimental GC, Mcclellan AL. The hydrogen bond. San Francisco, CA: Freeman; 1960. p. 136.
[56] Kenny JM, Maffezzoli A, Nicolais L. Modeling of the dynamic mechanical properties of semicrystalline thermoplastic matrix composites. Polym Composites 1992;13:386–93.
[57] Miller JA, Lin SB, Hwang KKS, Wu KS, Gibson PE, Cooper SL. Properties of polyether-polyurethane block copolymers: effects of hard segment length distribution. Macromolecules 1985;18:32–44.
[58] Garrett JT, Lin JS, Runt J. Influence of preparation conditions on microdomain formation in poly(urethane urea) block copolymers. Macromolecules 2002;35:161–8.
[59] Sternstein SS, Zhu A-J. Reinforcement mechanism of nanofilled polymer melts as elucidated by nonlinear viscoelastic behavior. Macromolecules 2002;35:7262–73.
[60] Chazeau L, Brown JD, Yanyo LC, Sternstein SS. Modulus recovery kinetics and other insights into the payne effect for filled elastomers. Polym Composites 2000;21:202–22.